Plasmon−Exciton Interactions Probed Using Spatial Coentrapment of Nanoparticles by Topological Singularities

Paul J. Ackerman,[†,‡] Haridas Mundoor,[†] Ivan I. Smalyukh,*[,†,‡,||,⊥] and Jao van de Lagemaat*[,§,†,⊥]

[†]Department of Physics, University of Colorado, Boulder, Colorado 80309, United States, [‡]Department of Electrical, Computer and Energy Engineering, University of Colorado, Boulder, Colorado 80309, United States, [§]National Renewable Energy Laboratory, Golden, Colorado 80401, United States, [||]Liquid Crystal Materials Research Center and Materials Science and Engineering Program, University of Colorado, Boulder, Colorado 80309, United States, and [⊥]Renewable and Sustainable Energy Institute, National Renewable Energy Laboratory and University of Colorado, Boulder, Colorado 80309, United States

ABSTRACT We study plasmon−exciton interaction by using topological singularities to spatially confine, selectively deliver, cotrap and optically probe colloidal semiconductor and plasmonic nanoparticles. The interaction is monitored in a single quantum system in the bulk of a liquid crystal medium where nanoparticles are manipulated and nanoconfined far from dielectric interfaces using laser tweezers and topological configurations containing singularities. When quantum dot-in-a-rod particles are spatially colocated with a plasmonic gold nanoburst particle in a topological singularity core, its fluorescence increases because blinking is significantly suppressed and the radiative decay rate increases by nearly an order of magnitude owing to the Purcell effect. We argue that the blinking suppression is the result of the radiative rate change that mitigates Auger recombination and quantum dot ionization, consequently reducing nonradiative recombination. Our work demonstrates that topological singularities are an effective platform for studying and controlling plasmon−exciton interactions.
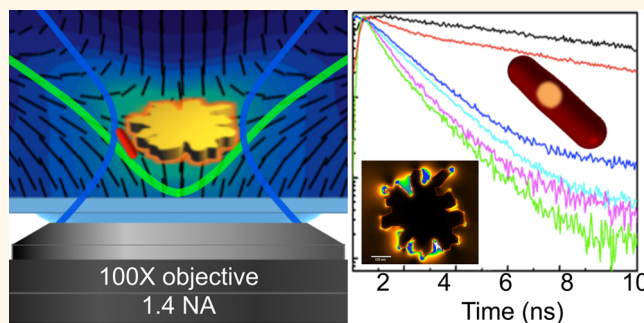
KEYWORDS: plasmonics · semiconductor nanocrystals · metal nanoparticles · topological singularities · blinking

The possibility of impacting the excited-state dynamics as well as the final fate of excitons by coupling excitons and surface plasmons, possibly leading to desirable outcomes such as increased singlet fission rates or multiple exciton generation, has been an active avenue of research.[1] Strong interactions causing Rabi splittings in the 100s of meV are possible between excitons in molecules or quantized nanosized semiconductors and surface plasmons.[2−5] These interactions can also be used in extremely sensitive single-molecule detection schemes.[6] The potential to influence excited-state energies and dynamics is of high interest to exert a measure of control in systems used in solar-to-electricity or solar-to-fuel photoconversion applications. Semiconductor quantum dots are often described as model systems for

excitonic behavior. Because of the size quantization, one can shift energy levels in order to, for example, turn-on-and-off singlet fission from molecules that can transfer charges to these nanoparticles.[7] Surface plasmons can have strong interaction with excitons on nearby colloidal quantum dots, and this interaction is an interesting approach to manipulating excited state energies.[2,8] One consistent observation when looking at light emission from semiconductor quantum dots is that their fluorescence blinks.[9,10] This phenomenon is generally attributed to the dot becoming charged, which makes it dark owing to Auger recombination, and discharging, giving rise to intermittent fluorescence.[9] A similar effect was observed in current flow through quantum dots trapped in the gap between tip and substrate in a tunneling microscope
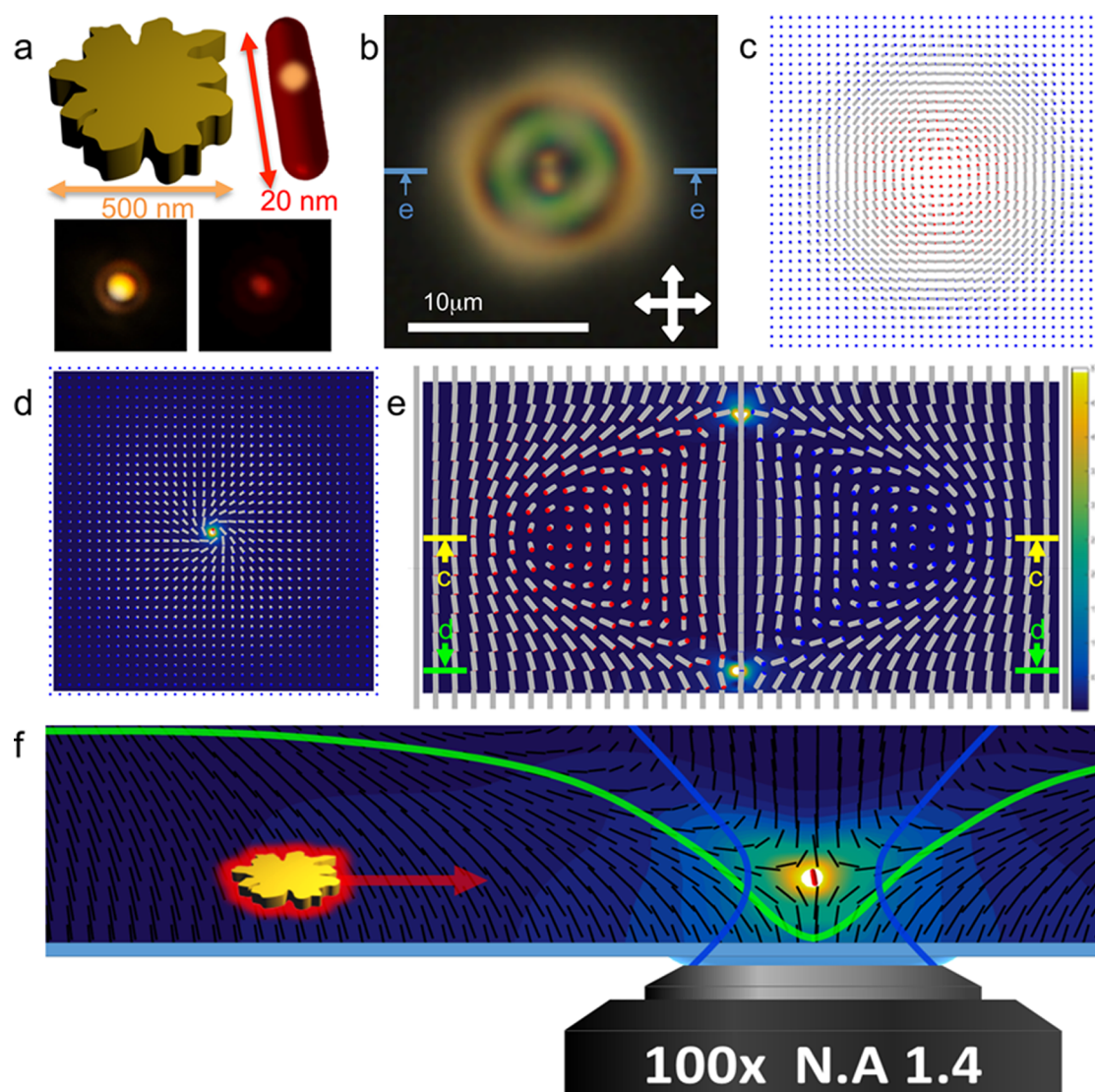
Figure 1. Topological singularities as elastic traps for metal and semiconductor nanoparticles. (a) Schematic of a NB (left) and QR (right). The micrographs beneath the schematics show a dark-field microscopy image of a single NB based on the strong scattering from it and a fluorescence image of a single quantum rod; both particles are imaged on a glass substrate. **(b)** Polarizing optical microscopy texture of a toron; double-headed white arrows depict orientations of polarizers. **(c)** Computer simulated director structure in the cell midplane, intersecting the toron in its solitonic equatorial plane, as denoted in (e) using yellow lines. **(d)** Computer simulated director structure within an in-plane cross-section passing through a point singularity of a toron, as denoted in (e), overlaid on the plot of the total elastic free energy density shown using a corresponding color scheme provided in the right-side inset in (e). **(e)** Computer simulated director structure in the vertical X−Z cross-section passing through the toron's central axis and its two hyperbolic point singularities, as denoted in (a) using blue lines. **(f)** Schematic representation of nanoinclusions interacting with the elastic potential (green curve) formed by a hyperbolic point singularity elastic trap, which is optically probed and observed through an objective lens.

and can be explained by the same effect.[11] It has been shown that it is possible to suppress the fluorescence blinking in quantum dots by controlling the chemical environment[12] and by growing thick, passivating shells around the core of the particles[13,14] giving rise to extraordinarily stable quantum emitters.

In this work, we demonstrate coupling to a nearby plasmonic particle as another way to decrease intermittency which, by increasing the radiative decay rate through the Purcell effect, increases the likelihood of radiative recombination *versus* ionization of the exciton or Auger recombination and therefore keeps the

fluorescent particle in its bright state more often and for longer periods of time. Similar experiments performed on single or assemblies of semiconducting nanocrystals with metal particle or metal surfaces show decrease in the fluorescence blinking;[15−21] however most of the experiments were not performed on the same semiconducting particles throughout the experiments.[16−18,20,21] We probe this effect in the bulk of a dielectric medium using a liquid crystal (LC) topological singularity, where we controllably bring a plasmonic particle in close proximity to a single semiconducting nanocrystal using a combination of noncontact optical

manipulation and elastic forces, which uniquely allows us to exclude the effects of proximity to substrates on which the plasmon−exciton interactions are typically studied.[19] This work also demonstrates that topological singularities can serve as an effective platform for studying plasmon−exciton interaction and that the fluorescence blinking of semiconducting nanocrystals can be effectively suppressed by using surface plasmons instead of surface passivation.

RESULTS AND DISCUSSION

Optical and Elastic Trapping of Nanoparticles. We use gold Nanoburst[22−24] (NB, obtained from Nanopartz Inc.) shaped as ∼500 nm discs with irregular sharp edges and dot-in-rod 5×20 nm CdSe/CdS quantum rod (QR) semiconducting nanocrystals with emission peak at 570 nm,[25,26] which are shown schematically and in optical micrographs in Figure 1a. Single NBs provide strong and localized field enhancement due to sharp features and are readily identified in dark-field microscopy as strong scattering yellow spots. The QRs that were used have good long-term stability in different chemical environments and can be uniquely identified and imaged based on fluorescence detected using a dichroic mirror and band-pass filter (see Supporting Information for details). These particles are dispersed in a chiral nematic LC host fluid at vanishingly low volume fractions (on the order of 1000 QRs and 10 000 NBs per 1 μL of the LC) and infiltrated into a LC cell. Spontaneous formation and laser generation of configurations known as torons[27] (Figure 1b) are reliably achieved in regions of cholesteric pitch to cell thickness $p/d \sim 1$ in such cells.

Our optical trapping system can manipulate NBs[23] and self-assembled toron structures with topological singularities,[28] but not the smaller QRs. This is consistent with the estimates of optical trapping forces as a function of particle dimensions, which show that optical gradient forces for such small QR nanoparticles are comparable in strength to Brownian motion.[29] We therefore control QRs with topological elastic traps of LC singularities that are free of this deficiency and can effectively entrap nanoparticles[22] and molecular self-assemblies.[30] As illustrated in Figure 1, we exploit the hyperbolic point singularities in a frustrated confined chiral nematic LC that are stabilized against annihilation by a solitonic double-twist-torus of a toron shown in a polarizing optical micrograph in Figure 1b. Numerical modeling of the director field of the toron structure (Figure 1d−f) illustrates a large elastic energy density associated with the two twist-bound hyperbolic point singularities, each resulting in a viable elastic trap. Furthermore, these distortions of the director field decay slowly in all lateral directions, so that attractive elastic forces act on particles at distances ∼10 μm much larger than their size[22] and much larger than the range of action of optical trapping forces,[29] thus mediating entrapment of the nanoinclusions that are originally found far from the trapping sites of the point singularities. In the cores of these energetically costly hyperbolic point singularities, the orientational ordering of the LC host is undefined within a volume of effective diameter 10−50 nm,[22] which is capable of entrapping even the particles that are too small to be trapped by laser tweezers.[29] By exploiting these properties of hyperbolic point elastic traps, we first localize QRs in the singular cores through elasticity-mediated interactions of the nanoinclusions with the singularities and then observe their fluorescence. Following this, NBs are brought to the vicinity of these point singularities containing QRs using the optical trapping system and then released (Figure 1f). Elastic attraction and eventual spatial confinement to the singularity core emerges from a combination of minimization of elastic free energy through sharing of director distortions and displacement of energetically costly LC with reduced orientational order.[22] This results in nanoscale localization and coentrapment of QRs and NBs, allowing us to compare fluorescence of the same QRs when they are entrapped in the singularity alone with the fluorescence of the QRs in close proximity to plasmonic NBs during coentrapment at the latter stage of this experiment.

To characterize topological elastic trapping of nanoparticles, the NB-singularity interaction was probed with video microscopy (Figure 2). Frames 1−3 of Figure 2a show the NB manipulated by our optical trapping system. Frames 4−7 of Figure 2a reveal the attractive NB-singularity elastic interaction after the NB is released near one of the point singularities of a toron. Using dark-field video microscopy, we optically track the NB far from singularities (free diffusion), as it is pulled into a topological elastic trap and also once it is trapped in a singularity. We derive the elastic interaction potential and elastic trap potential. The erratic 2D free diffusion trajectory (Figure 2b) in a uniformly vertically aligned LC yields the viscous drag coefficient c_d. Since this system is in the regime of low Reynolds number (Re $\ll 10^{-7}$),[22] inertia effects are negligible and the NB-singularity elastic attractive force F_{el} is balanced by the viscous drag force, $F_d = c_d v(t)$, where $v(t) = dr_{cc}/dt$ and r_{cc} is the NB-singularity time dependent center-to-center separation (Figure 2b). The elastic interaction potential is then calculated by integrating F_{el} obtained from this force balance (Figure 2b). By tracking the NB trapped by the singularity (Figure 2c), we construct a histogram of NB displacements, from which we derive the elastic trap potential by assuming a simple harmonic potential attraction model near the equilibrium location.[28] This reveals that the center of the NB is confined within a volume of effective radius smaller than 100 nm.

Plasmon−Exciton Interaction. To probe the photo physics of QRs, torons containing only QRs in only one of their singularities are illuminated with a mercury lamp
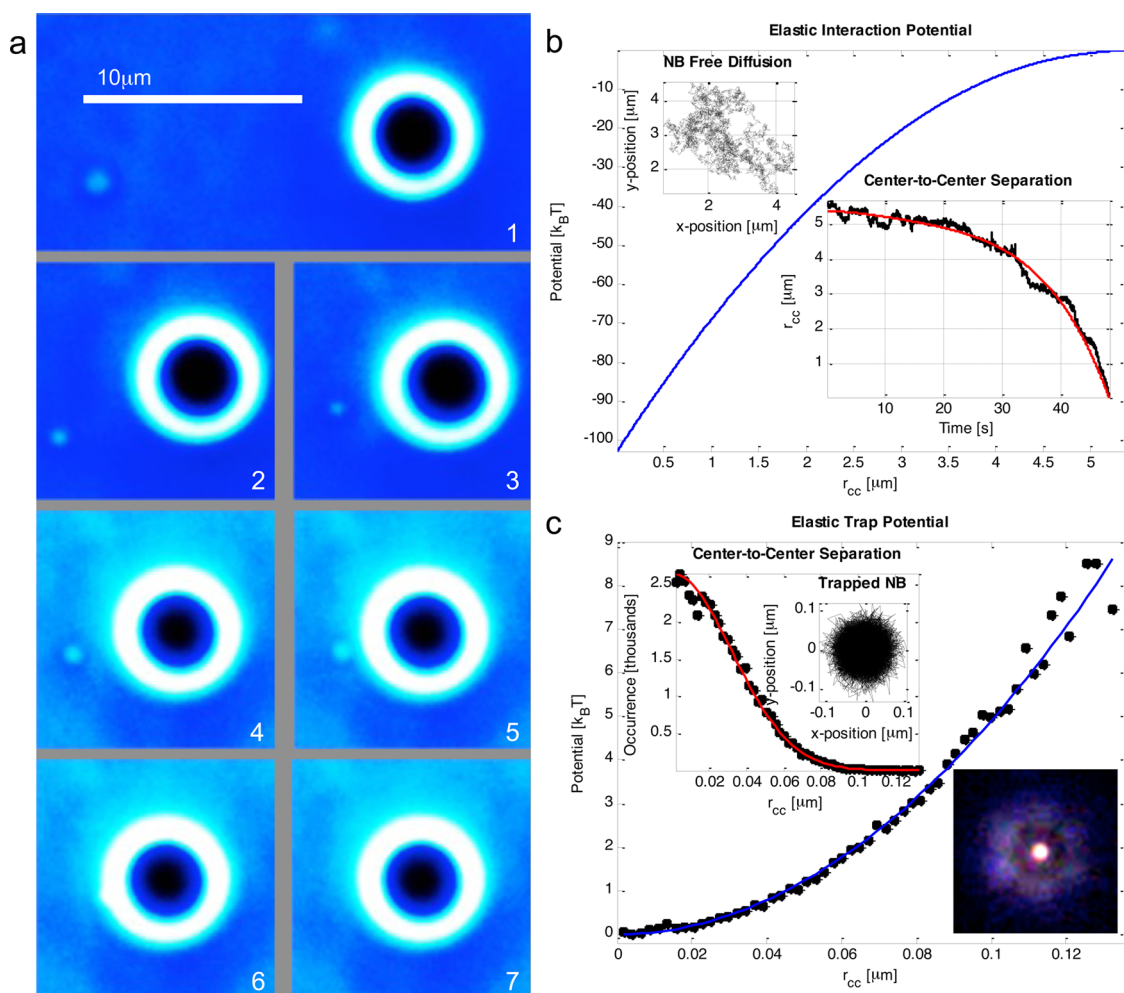
Figure 2. Release from optical traps, elastic interaction, and entrapment of nanoparticles in a topological point singularity. (a) Optical and elastic trapping of a NB (small bright spot) nearby a toron (visible as large bright ring of enhanced light scattering). Frames 1—3 show optical manipulation of the NB to a desired initial location near the toron and close to one of the substrates substrate. Frames 4—7 show the NB elastically pulled toward the toron center after its release from the laser trap. **(b)** Elastic interaction potential *versus* the center-to-center separation (r_{cc}) between the NB and toron singularity (blue curve), derived from the bottom-right inset plots of r_{cc} *versus* time and using the NB diffusion constant obtained from probing free diffusion (top-left inset). **(c)** Trapping potential and stiffness characterized *via* tracking the singularity-entrapped NB. The trapping potential is derived from the r_{cc} histogram shown in the top-left inset. The bottom-right inset image shows the NB particle entrapped by a toron singularity as observed in dark-field mode (the inset edge length is ≈5 μm). The characteristic stiffness of a toron singularity elastic trap is ~4 × 10^{-3} pN/nm.

and the resulting fluorescence is monitored. Figure 3a and 3b show bright field micrographs of such a toron with a QR in the "ON" and "OFF" state, respectively. Then, to probe the effects of plasmon—exciton interaction on these QR properties, the NB is cotrapped by the point singularity according to the procedure described above. Computer simulations (Figure 3c—e) reveal the electromagnetic field enhancement by the NB at wavelengths 570 nm, 950 and 473 nm, which are the emission and two excitation wavelengths used in the experiments discussed below. Consistently, the QR emission increases (Figure 3f,g), as seen from comparing time-averaged frames of two torons with QR particles before and after coentrapping the NB in the point singularity (top right). To analyze the corresponding blinking characteristics of QRs, we record fluorescence trajectories using 473 nm diode laser illumination and Avalanche

photo diode (APD) with a binning time of 10 ms. Figure 4a,b show characteristic fluorescence trajectories of QRs before and after introducing a NB particle into the elastic trap. It is clear that QR particles stay predominantly in the "ON" state after cotrapping NBs in the LC singularity. It should be noted that the blinking trajectories are affected by the diffusion of the particles, resulting in slight intensity fluctuations due to displacement of the particles from the focal plane. The effects of introducing the NB are clearly visible from the histogram plotted in the right-side insets of Figure 4a,b, showing a change in the blinking statistics. Further, we have performed detailed analysis of the blinking following the constant thresholding[20,31,32] and change point analysis methods reported recently,[33] where we have calculated the probability density for the "ON" and "OFF" times (Figure 4c—f). The results of our analysis using
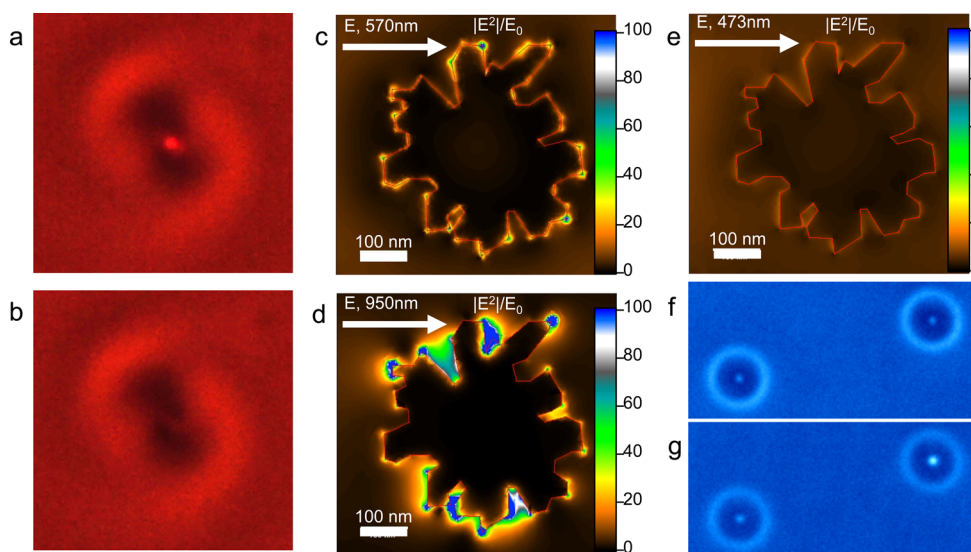
Figure 3. Fluorescence enhancement and blinking of QRs without and with NB coentrapment. (a,b) Bright field micrographs depicting the fluorescence signal of a QR elastically trapped in a toron point singularity while in the "ON" (a) and "OFF" (b) states. **(c−e)** Computer-simulated electromagnetic field enhancement around NBs calculated at 570, 950 and 473 nm excitation wavelengths of the incident light with linear polarization (vibration direction of the light's electric field E) by a NB in the LC medium. **(f,g)** Time averaged image of QRs elastically trapped in torons before (f) and after (g) introducing a NB into the toron on the right.
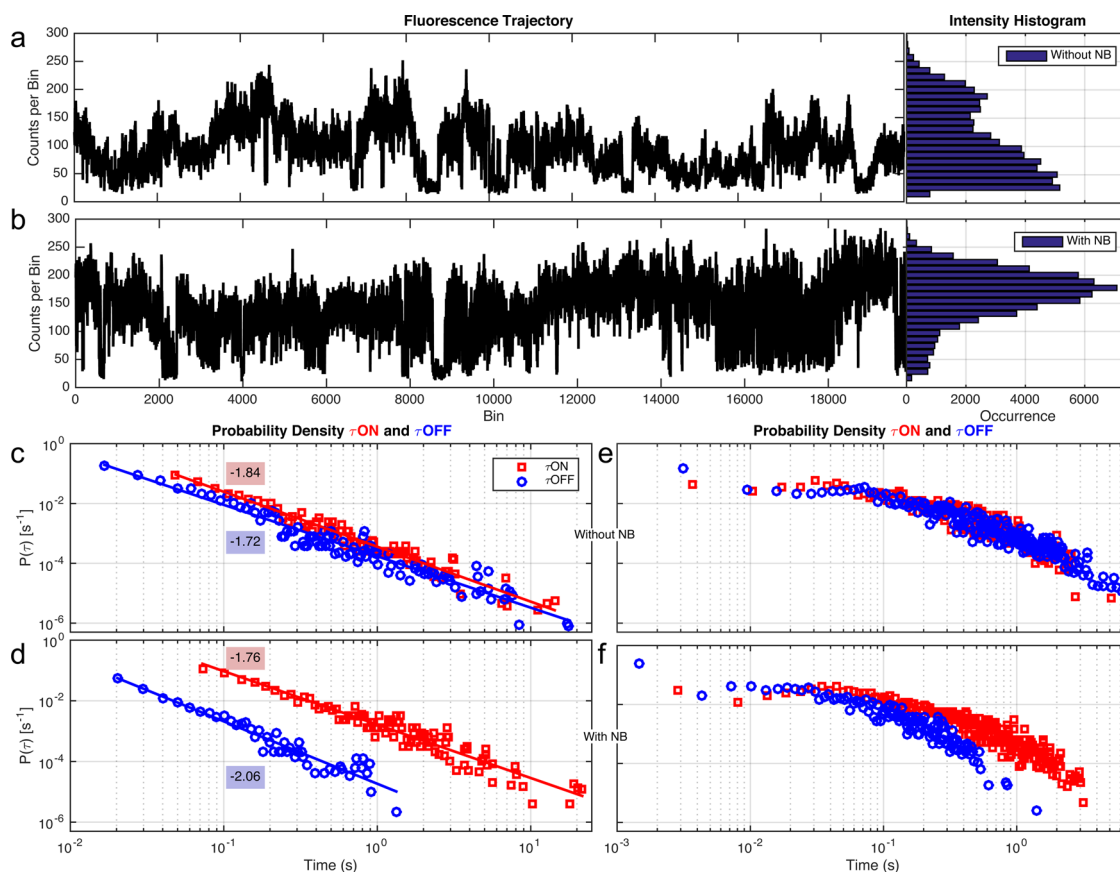

Figure 4. Characterization of fluorescence intermittency of QRs before and after introducing plasmonic NBs. (a,b) Fluorescence time traces of QRs elastically trapped in a toron point singularity without (a) and with (b) the NB particle in the elastic trap. The "ON" and "OFF" times of the QRs is represented by the corresponding histograms in the right-side insets. Analysis of fluorescence time trace with constant thresholding (c,d) and using the change point analysis method (e,f) for the curves displayed in (a) and (b) and corresponding to (c,e) the QRs alone and (d,f) in the close neighborhood of NBs. Here $\rho(\tau)$ is probability density defined as in reference 32 and plotted as $\rho(\tau ON)$ and $\rho(\tau OFF)$ for on and off times (red squares and blue circles, respectively). τON and τOFF are time periods of sustained fluorescence emission and darkness, respectively.
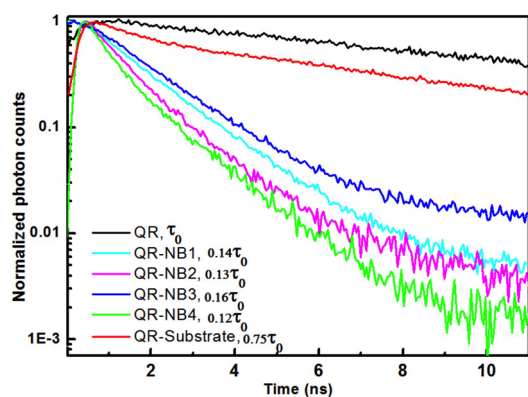
Figure 5. Characterization of fluorescence lifetime of QRs. Photoluminescence decay for QRs entrapped in a toron's point singularity (black curve) and when placed on a glass substrate (red curve) are compared to four sets of characteristic decay curves for QRs in topological point singularities coentrapped with the NB (blue, cyan, magenta and green curves). The fluorescence lifetime for QRs measured in the topological elastic trap is $\tau_0 \approx 10.16$ ns.

the former method are consistent with the earlier reports[20,31,32] showing typical power-law behavior of such data (Figure 4c,e) and that the particle is far more often in the "ON" state in the presence of plasmonic enhancement than without it. The same is concluded from the change-point analysis (Figure 4d,f). The probability density of "ON" states of QRs in the presence of a NB increases, indicating decreased blinking and prevalence of the "ON" state.

To get additional insights into the nature of plasmon–exciton interactions, we have performed fluorescence lifetime measurements of QRs located inside a point singularity, before and after introducing the NBs. For this, the excitation of the system was realized through a two photon absorption process using 950 nm light from a pulsed Ti:sapphire laser. Although the accuracy of lifetime measurements is somewhat limited by the repetition rate of our laser (80 MHz), the comparison of the decay curves unambiguously shows that the photoluminescence from the QR decays much faster in the presence of NBs than when QR are entrapped alone or on a dielectric substrate (Figure 5). The excited-state lifetime for the QR isolated through trapping within the topological singularity in the bulk of the dielectric LC medium is ≈10.16 ns. Introduction of a NB into the trap for different experiments with different nanoparticles repeatedly results in a dramatic change of this lifetime by a factor ranging from 0.12 to 0.16, yielding lifetimes within 1.2–1.6 ns. The somewhat broad range of lifetime values observed for different QR-NB combinations is likely due to the irregular shapes of the NBs and different specific locations/orientations of the QRs relative to the NBs, as well as variations in the illumination light's propagation direction relative to the QR-NB system. The blinking experiments were consistently performed on one and the same QR before and after introducing a NB,

the fluorescence lifetimes were measured for a series of QR-NB assemblies produced in the toron's point defects in each case comparing the same QR before and after addition of a NB particle. Importantly, the observed dramatic effect of plasmon-exciton interaction on the fluorescence lifetime is separated from the effect of surface proximity to a dielectric substrate such as glass, which results in a much smaller decrease of the fluorescence lifetime by ≈25% (Figure 5).

Our experimental finding of nearly an order of magnitude increase in the fluorescence rate of QRs upon adding the plasmonic NB to an elastic trap is consistent with the Purcell effect, owing to the increased density of final states for photon emission in the presence of the NB.[34−37] Such an effect also explains the decrease in blinking. The intensity of the emission for the "ON" state is not strongly affected and since the QR particle is 10−20 nm from the NB surface, where nonradiative rates are only marginally affected,[35] one does not expect to observe any significant quenching of the fluorescence. Second, the field enhancement produced by a NB at the excitation wavelength used for blinking experiments (Figure 3e) is small and has minimal effect on the excitation rate of QRs. The coupling of the QR emission to the plasmon modes of the NBs influences the fluorescence blinking by reducing the probability of the dark exciton generation and by driving the branching of the excited states of the QR to light emission instead of charge carrier trapping. This keeps the QRs predominantly in the "ON" state instead of the ionized "OFF" state. Similar but usually smaller enhancements of the fluorescence decay and suppression of blinking have been observed before in chemically pre-engineered nanoparticles with plasmonic resonator shells around the quantum dot,[17,18] quantum dots immobilized on plasmonic substrates[16,38] and in engineered quantum dot/plasmonic particle dimers.[39] In these experiments, however, the effect of the plasmonic field cannot be probed using the same quantum dots at different experimental stages, making it difficult to unequivocally prove that the effect is due to the plasmonic particle's presence. In contrast, in a similar experiment to ours,[19] a plasmonic particle was brought closer to a colloidal core/shell quantum dot on a glass substrate using an AFM tip and a reversible suppression of blinking and a decrease of the fluorescence lifetime comparable to that described here was observed, albeit the surface proximity could have additionally influenced this behavior and in a different study,[15] a strong modification of nonradiative rates leading to quenching of the photoluminescence and concomitant suppression of blinking was observed when a gold particle suspended on a tip was brought into closer proximity than used in this paper to a quantum dot. In that case the suppression of blinking was due to an increase in nonradiative rates which also would lead to

a decrease in ionization events. In the current paper, we show that this effect can be seen even for the same plasmonic-quantum nanoparticle system *suspended* in its entirety in a fluid medium bulk, where the plasmonic field was specifically brought to the quantum nanoparticle by "soft" self-assembly methods instead of external forces. While the sharp edges of the NB help to localize the electromagnetic field very strongly and help make the NB easy to move using laser tweezers, the randomness of the shape of the NB limits our knowledge of the QR position and orientation relative to NB enhancement field, resulting in variations in the plasmon—exciton interaction for each individual NB-QR combination and somewhat limiting the possibility of further quantifying the effect, which will be the goal of our future studies.

Interestingly, with the exception of rare cases, coentrapment of QRs and NBs in the topological point singularities is such that the fluorescence of QRs is enhanced, the lifetime decreases, and the "ON" states are more prevalent. This may imply that the QRs are entrapped in the region of elastic distortions around the somewhat bigger NB rather than physically touching it, in which case one would expect quenching of fluorescence. Although chemical methods allow for producing nanostructures with well-defined distance between plasmonic metal and semiconductor components pre-engineered to provide enhancement,[40,41] it is interesting that the NB-QR nanostructures achieve this through elasticity-mediated self-assembly driven by the LC topological singularity. This, along with the recent progress in generating stable arrays of topological singularities,[42,43] opens opportunities of mass-producing LC-based nanostructured materials with arrays of singularities and self-assembled metal—semiconductor nanostructures with pre-engineered plasmon—exciton interactions and the ensuing new physical properties. We also note that the conditions for plasmon—exciton interactions studied here have not been optimized for particular outcomes of potential interest, such as maximization of fluorescence "ON" time or shortening of photoluminescence lifetime. However, the comparison of computer-simulated plasmonic field enhancement at different wavelengths (Figure 3), combined with preselected spectral characteristics of quantum rods or dots, shows ample possibilities for engineering the physical behavior of such nanostructured self-assembled systems, which we will pursue in future studies.

CONCLUSIONS

We have demonstrated that topological singularities can be used to coentrap quantum nanorods and plasmonic nanoparticles within a highly localized volume of a dielectric LC medium, overcoming limitations of laser manipulation techniques that lack the ability to trap quantum dots. This allows us to study plasmon—exciton interactions within the bulk of the LC fluid, unaffected by the interaction with substrates. Moreover, trapping of the nanoparticles in LC topological singularities allows us to probe effects of plasmon—exciton interactions through characterizing fluorescence of the same semiconducting particle before and after introducing the plasmonic particle. Characterization of emission properties of studied quantum rods before and after coentrapment with plasmonic nanoparticles indicates an order of magnitude decrease in the fluorescence lifetime, consistent with the Purcell effect, enhanced brightness and an increased persistence of the "ON" state. Our findings not only enhance the current understanding of plasmon—exciton interactions but also point to the possibility for exploiting such interactions in designed self-assembled mesostructured composite materials with pre-engineered physical behavior. Furthermore, considering the facile response of liquid crystals to external fields and light,[44] such interactions and the ensuing composites can be dynamic and reconfigurable.

MATERIALS AND METHODS

Chiral Nematic LC Preparation. We mix 4-cyano-4′-pentylbiphenyl (5CB) nematic host (Chengzhi Younghua Display Material Co., Ltd.) with a chiral agent, either CB15 (EM Industries) or cholesteryl pelargonate (Sigma-Aldrich). The desired cholesteric pitch p, the distance over which the LC ground state director twists by 2π, is defined by controlling the composition of the LC mixture according to the relation $p = 1/(|H_{HTP}| \cdot C_{agent})$, where H_{HTP} is the helical twisting power in 5CB (7.3 μm^{-1} for right-handed CB15 and -6.25 μm^{-1} for left-handed cholesteryl pelargonate where the $\pm$ sign denotes the corresponding right/left handedness) and C_{agent} is the concentration of the chiral additive in the nematic host. All experiments are performed using LCs with $p \approx 8$ μm and the handedness was found to play no role in the following experiments. By mixing the LC with either NBs dispersed in ethanol or QRs in toluene and then slowly evaporating the solvent at 65 °C, we prepare two separate NB-LC and QR-LC colloidal nanoparticle dispersions, as needed for the experiments described above.

LC Cell Fabrication. LC cells were assembled using glass plates treated with Dimethyl octadecyl [3-(trimethoxysilyl) propyl] ammonium chloride (Sigma-Aldrich) to obtain strong perpendicular surface boundary conditions for the LC director describing the local average orientation of rod-like molecules. Wedge cells with thickness $d = 7-10$ μm were produced by spacing two substrates with glass fiber segments of diameter 7 and 10 μm in UV-curable glue at the opposite ends of the cell. The dihedral angle between the substrates was kept below 3 degrees such that the local thickness variation can be neglected. The LC mixtures were coinfused into the cell by capillary forces at 75 °C, rapidly cooled to room temperature and sealed with fast-setting epoxy.

Experimental Setup and Procedures. The experimental setup was built around an inverted microscope IX81 (Olympus). The optical trapping system, used for noncontact optical manipulation of NBs and torons, is based on a diode laser (1,064 nm, from LaserGlow).[22,23] Excitation of QRs is done using a mercury lamp, a 473 nm diode laser (from LaserGlow) or pulsed excitation from a tunable Ti:sapphire oscillator (Chameleon Ultra II, Coherent, 140 fs, 80 MHz, used at 950 nm) and the fluorescence signal is detected using an Avalanche photo diode (APD, Picoquant). Fluorescence is detected through a confocal

pinhole and filtered by a band-pass filter (centered at 610 nm, 75 nm bandwidth, from Chroma Technology Corp.). Light is focused by an aspheric lens to the active area of the APD connected to a data acquisition board (NIDAQ-6363, National Instruments) and photon counting hardware (SPC-130, Becker & Hickl GmbH). We use a 100× oil immersion objective with adjustable numerical aperture (NA) of 0.6−1.3, an electron multiplying charge coupled device (EMCCD, iXon3 888, Andor Technology) and a CCD camera (Flea, PointGrey) for imaging. Dark-field imaging is achieved by adjusting the NA of the 100× objective to be smaller than the NA of a dark-field condenser, allowing us to visualize strong scattering of individual NBs, which we use for tracking of these nanoparticles. The fluorescence blinking of QRs is analyzed based on the thresholding method and also using a change-point algorithm,[45] as discussed in more detail in the Supporting Information.

Numerical Modeling. Equilibrium LC director configurations are modeled through minimization of elastic free energy[28] (Figure 1c−e) assuming strong perpendicular surface boundary conditions (see Supporting Information for details). Elastic constants of 5CB and experimental geometric parameters such as $d/p = 0.9$ are used in this modeling. The electromagnetic field enhancement of NBs in LCs is simulated using commercially available software (COMSOL Multiphysics), which is based on the finite element method, with a detailed description of the simulation approach provided in Reference.[23] Briefly, the incident electromagnetic wave passes through the computational volume from above (Z direction) along the orientation of the LC director. The simulation is done over a cylindrical volume with the lateral diameter of 1.5 μm and height of 1 μm, with the NB located at the center, enclosed between perfectly matched layers in the radial directions and optical "ports" in the vertical direction of the cylindrical volume. The simulations were performed at the two excitation wavelengths as well as the emission wavelength of the QRs.

Conflict of Interest: The authors declare no competing financial interest.

Supporting Information Available: The Supporting Information is available free of charge on the ACS Publications website at DOI: 10.1021/acsnano.5b05715.

Description of our implementation of the change point analysis of fluorescence blinking of QRs, details of numerical modeling of director structures and the corresponding elastic free energy landscapes, as well as additional details of experimental instrumentation utilized in our studies. Material parameters of 5CB used in numerical modeling. (PDF)

Movie showing fluorescence blinking of QDs when located on a glass substrate. (AVI)

Movies showing fluorescence blinking of QDs when entrapped by the topological singularity in a bulk of the LC fluid. (AVI)

REFERENCES AND NOTES

1. Johnson, J. C.; Reilly, T. H.; Kanarr, A. C.; van de Lagemaat, J. The Ultrafast Photophysics of Pentacene Coupled to Surface Plasmon Active Nanohole Films. *J. Phys. Chem. C* **2009**, *113*, 6871–6877.

2. Gómez, D. E.; Vernon, K. C.; Mulvaney, P.; Davis, T. J. Coherent Superposition of Exciton States in Quantum Dots Induced by Surface Plasmons. *Appl. Phys. Lett.* **2010**, *96*, 73108.

3. Gómez, D. E.; Vernon, K. C.; Mulvaney, P.; Davis, T. J. Surface Plasmon Mediated Strong Exciton-Photon Coupling in Semiconductor Nanocrystals. *Nano Lett.* **2010**, *10*, 274–278.

4. Cade, N. I.; Ritman-Meer, T.; Richards, D. Strong Coupling of Localized Plasmons and Molecular Excitons in Nanostructured Silver Films. *Phys. Rev. B: Condens. Matter Mater. Phys.* **2009**, *79*, 241404.

5. Symonds, C.; Bonnand, C.; Plenet, J. C.; Bréhier, A.; Parashkov, R.; Lauret, J. S.; Deleporte, E.; Bellessa, J. Particularities of Surface Plasmon−Exciton Strong Coupling with Large Rabi Splitting. *New J. Phys.* **2008**, *10*, 065017.

6. Zhao, J.; Sherry, L. J.; Schatz, G. C.; Van Duyne, R. P. Molecular Plasmonics: Chromophore-Plasmon Coupling and Single-Particle Nanosensors. *IEEE J. Sel. Top. Quantum Electron.* **2008**, *14*, 1418–1429.

7. Thompson, N. J.; Wilson, M. W. B.; Congreve, D. N.; Brown, P. R.; Scherer, J. M.; Bischof, T. S.; Wu, M.; Geva, N.; Welborn, M.; Voorhis, T. V.; *et al.* Energy Harvesting of Non-Emissive Triplet Excitons in Tetracene by Emissive PbS Nanocrystals. *Nat. Mater.* **2014**, *13*, 1039–1043.

8. Pelton, M. Modified Spontaneous Emission in Nanophotonic Structures. *Nat. Photonics* **2015**, *9*, 427–435.

9. Efros, A. L. Nanocrystals: Almost Always Bright. *Nat. Mater.* **2008**, *7*, 612–613.

10. Galland, C.; Ghosh, Y.; Steinbrück, A.; Sykora, M.; Hollingsworth, J. A.; Klimov, V. I.; Htoon, H. Two Types of Luminescence Blinking Revealed by Spectroelectrochemistry of Single Quantum Dots. *Nature* **2011**, *479*, 203–207.

11. Maturova, K.; Nanayakkara, S.; Luther, J. M.; van de Lagemaat, J. Fast Current Blinking in Individual PbS and CdSe Quantum Dots. *Nano Lett.* **2013**, *13*, 2338–2345.

12. Fomento, V.; Nesbitt, D. J. Solution Control of Radiative and Nonradiative Lifetimes: A Novel Contribution to Quantum Dot Blinking Suppression. *Nano Lett.* **2008**, *8*, 287–293.

13. Wang, X.; Ren, X.; Kahen, K.; Hahn, M. A.; Rajeswaran, M.; Maccagnano-Zacher, S.; Silcox, J.; Cragg, G. E.; Efros, A. L.; Krauss, T. D. Non-Blinking Semiconductor Nanocrystals. *Nature* **2009**, *459*, 686–689.

14. Mahler, B.; Spinicelli, P.; Buil, S.; Quelin, X.; Hermier, J.-P.; Dubertret, B. Towards Non-Blinking Colloidal Quantum Dots. *Nat. Mater.* **2008**, *7*, 659–664.

15. Bharadwaj, P.; Novotny, L. Robustness of Quantum Dot Power-Law Blinking. *Nano Lett.* **2011**, *11*, 2137–2141.

16. Fu, Y.; Zhang, J.; Lakowicz, J. R. Suppressed Blinking in Single Quantum Dots (QDs) Immobilized near Silver Island Films (SIFs). *Chem. Phys. Lett.* **2007**, *447*, 96–100.

17. Ji, B.; Giovanelli, E.; Habert, B.; Spinicelli, P.; Nasilowski, M.; Xu, X.; Lequeux, N.; Hugonin, J.; Marquier, F.; Greffet, J.; *et al.* Non-Blinking Quantum Dot with a Plasmonic Nanoshell Resonator. *Nat. Nanotechnol.* **2015**, *10*, 170–175.

18. Karan, N.; Keller, A.; Sampat, S.; Roslyak, O.; Arefin, A.; Hanson, C.; Casson, J.; Desireddy, A.; Ghosh, Y.; Piryatinski, A.; *et al.* Plasmonic Giant Quantum Dots: Hybrid Nanostructures for Truly Simultaneous Optical Imaging, Photothermal Effect and Thermometry. *Chem. Sci.* **2015**, *6*, 2224–2236.

19. Ratchford, D.; Shafiei, F.; Kim, S.; Gray, S. K.; Li, X. Manipulating Coupling between a Single Semiconductor Quantum Dot and Single Gold Nanoparticle. *Nano Lett.* **2011**, *11*, 1049–1054.

20. Shimizu, K.; Neuhauser, R.; Leatherdale, C.; Empedocles, S.; Woo, W.; Bawendi, M. Blinking Statistics in Single Semiconductor Nanocrystal Quantum Dots. *Phys. Rev. B: Condens. Matter Mater. Phys.* **2001**, *63*, 205316.

21. Shimizu, K. T.; Woo, W. K.; Fisher, B. R.; Eisler, H. J.; Bawendi, M. G. Surface-Enhanced Emission from Single Semiconductor Nanocrystals. *Phys. Rev. Lett.* **2002**, *89*, 117401.

22. Senyuk, B.; Evans, J. S.; Ackerman, P. J.; Lee, T.; Manna, P.; Vigderman, L.; Zubarev, E. R.; van de Lagemaat, J.; Smalyukh, I. I. Shape-Dependent Oriented Trapping and Scaffolding of Plasmonic Nanoparticles by Topological Defects for Self-Assembly of Colloidal Dimers in Liquid Crystals. *Nano Lett.* **2012**, *12*, 955–963.

23. Mundoor, H.; Lee, T.; Gann, D. G.; Ackerman, P. J.; Senyuk, B.; van de Lagemaat, J.; Smalyukh, I. I. Optically and Elastically Assembled Plasmonic Nanoantennae for Spatially Resolved Characterization of Chemical Composition in Soft Matter Systems Using Surface Enhanced Spontaneous and Stimulated Raman Scattering. *J. Appl. Phys.* **2014**, *116*, 063511.

24. Senyuk, B.; Glugla, D.; Smalyukh, I. I. Rotational and Translational Diffusion of Anisotropic Gold Nanoparticles in Liquid Crystals Controlled by Varying Surface Anchoring. *Phys. Rev. E* **2013**, *88*, 062507.

25. Smith, E. R.; Luther, J. M.; Johnson, J. C. Ultrafast Electronic Delocalization in CdSe/CdS Quantum Rod Heterostructures. *Nano Lett.* **2011**, *11*, 4923–4931.

26. Talapin, D. V.; Koeppe, R.; Götzinger, S.; Kornowski, A.; Lupton, J. M.; Rogach, A. L.; Benson, O.; Feldmann, J.; Weller, H. Highly Emissive Colloidal CdSe/CdS Heterostructures of Mixed Dimensionality. *Nano Lett.* **2003**, *3*, 1677–1681.

27. Smalyukh, I. I.; Lansac, Y.; Clark, N. A.; Trivedi, R. P. Three-Dimensional Structure and Multistable Optical Switching of Triple-Twisted Particle-like Excitations in Anisotropic Fluids. *Nat. Mater.* **2010**, *9*, 139–145.

28. Ackerman, P. J.; van de Lagemaat, J.; Smalyukh, I. I. Self-Assembly and Electrostriction of Arrays and Chains of Hopfion Particles in Chiral Liquid Crystals. *Nat. Commun.* **2015**, *6*, 6012.

29. Ashkin, A.; Dziedzic, J. M.; Bjorkholm, J. E.; Chu, S. Observation of a Single-Beam Gradient Force Optical Trap for Dielectric Particles. *Opt. Lett.* **1986**, *11*, 288–290.

30. Wang, X.; Miller, D. S.; Bukusoglu, E.; de Pablo, J. J.; Abbott, N. L. Topological Defects in Liquid Crystals as Templates for Molecular Self-Assembly. *Nat. Mater.* **2015**, DOI: 10.1038/nmat4421.

31. Crouch, C. H.; Sauter, O.; Wu, X.; Purcell, R.; Querner, C.; Drndic, M.; Pelton, M. Facts and Artifacts in the Blinking Statistics of Semiconductor Nanocrystals. *Nano Lett.* **2010**, *10*, 1692–1698.

32. Kuno, M.; Fromm, D. P.; Hamann, H. F.; Gallagher, A.; Nesbitt, D. J. Nonexponential "blinking" Kinetics of Single CdSe Quantum Dots: A Universal Power Law Behavior. *J. Chem. Phys.* **2000**, *3117*, 3117–3120.

33. Schmidt, R.; Krasselt, C.; Göhler, C.; Von Borczyskowski, C. The Fluorescence Intermittency for Quantum Dots Is Not Power-Law Distributed: A Luminescence Intensity Resolved Approach. *ACS Nano* **2014**, *8*, 3506–3521.

34. Song, J.; Atay, T.; Shi, S.; Urabe, H.; Nurmikko, A. V. Large Enhancement of Fluorescence Efficiency from CdSe/ZnS Quantum Dots Induced by Resonant Coupling to Spatially Controlled Surface Plasmons. *Nano Lett.* **2005**, *5*, 1557–1561.

35. Anger, P.; Bharadwaj, P.; Novotny, L. Enhancement and Quenching of Single-Molecule Fluorescence. *Phys. Rev. Lett.* **2006**, *96*, 113002.

36. Govorov, A. O.; Bryant, G. W.; Zhang, W.; Skeini, T.; Lee, J.; Kotov, N. A.; Slocik, J. M.; Naik, R. R. Exciton-Plasmon Interaction and Hybrid Excitons in Semiconductor-Metal Nanoparticle Assemblies. *Nano Lett.* **2006**, *6*, 984–994.

37. Kühn, S.; Håkanson, U.; Rogobete, L.; Sandoghdar, V. Enhancement of Single-Molecule Fluorescence Using a Gold Nanoparticle as an Optical Nanoantenna. *Phys. Rev. Lett.* **2006**, *97*, 017402.

38. Wu, X.-W.; Gong, M.; Dong, C.-H.; Cui, J.-M.; Yang, Y.; Sun, F.-W.; Guo, G.-C.; Han, Z.-F. Anti-Bunching and Luminescence Blinking Suppression from Plasmon-Interacted Single CdSe/ZnS Quantum Dot. *Opt. Express* **2010**, *18*, 6340–6346.

39. Cohen-Hoshen, E.; Bryant, G. W.; Pinkas, I.; Sperling, J.; Bar-joseph, I. Exciton−Plasmon Interactions in Quantum Dot−Gold Nanoparticle Structures. *Nano Lett.* **2012**, *12*, 4260–4264.

40. Liu, N.; Prall, B. S.; Klimov, V. I. Hybrid Gold/Silica/Nanocrystal-Quantum-Dot Superstructures: Synthesis and Analysis of Semiconductor-Metal Interactions. *J. Am. Chem. Soc.* **2006**, *128*, 15362–15363.

41. Khanal, B. P.; Pandey, A.; Li, L.; Lin, Q.; Bae, W. K.; Luo, H.; Klimov, V. I.; Pietryga, J. M. Generalized Synthesis of Hybrid Metal-Semiconductor Nanostructures Tunable from the Visible to the Infrared. *ACS Nano* **2012**, *6*, 3832–3840.

42. Evans, J. S.; Ackerman, P. J.; Broer, D. J.; van de Lagemaat, J.; Smalyukh, I. I. Optical Generation, Templating, and Polymerization of Three-Dimensional Arrays of Liquid-Crystal Defects Decorated by Plasmonic Nanoparticles. *Phys. Rev. E* **2013**, *87*, 032503.

43. Ackerman, P. J.; Qi, Z.; Smalyukh, I. I. Optical Generation of Crystalline, Quasicrystalline, and Arbitrary Arrays of Torons in Confined Cholesteric Liquid Crystals for Patterning of Optical Vortices in Laser Beams. *Phys. Rev. E* **2012**, *86*, 021703.

44. Liu, Q.; Yuan, Y.; Smalyukh, I. I. Electrically and Optically Tunable Plasmonic Guest-Host Liquid Crystals with Long-Range Ordered Nanoparticles. *Nano Lett.* **2014**, *14*, 4071–4077.

45. Watkins, L. P.; Yang, H. Detection of Intensity Change Points in Time-Resolved Single-Molecule Measurements. *J. Phys. Chem. B* **2005**, *109*, 617–628.